Contrib Mineral Petrol (2010) 159:371–387
DOI 10.1007/s00410-009-0432-3

ORIGINAL PAPER

The time scales of magma mixing and mingling involving primitive melts and melt–mush interaction at mid-ocean ridges

Fidel Costa · Laurence A. Coogan · Sumit Chakraborty

Received: 19 February 2009 / Accepted: 29 July 2009 / Published online: 14 August 2009

Abstract We have studied the chemical zoning of plagioclase phenocrysts from the slow-spreading Mid-Atlantic Ridge and the intermediate-spreading rate Costa Rica Rift to obtain the time scales of magmatic processes beneath these ridges. The anorthite content, Mg, and Sr in plagioclase phenocrysts from the Mid-Atlantic Ridge can be interpreted as recording initial crystallisation from a primitive magma (~11 wt% MgO) in an open system. This was followed by crystal accumulation in a mush zone and later entrainment of crystals into the erupted magma. The initial magma crystallised plagioclase more anorthitic than those in equilibrium with any erupted basalt. Evidence that the crystals accumulated in a mush zone comes from both: (1) plagioclase rims that were in equilibrium with a Sr-poor melt requiring extreme differentiation; and (2) different crystals found in the same thin section having different histories. Diffusion modelling shows that crystal residence times in the mush were <140 years, whereas the interval between mush disaggregation and eruption was ≤1.5 years. Zoning of anorthite content and Mg in plagioclase phenocrysts from the Costa Rica Rift show that they partially or completely equilibrated with a MgO-rich melt (>11 wt%). Partial equilibration in some crystals can be modelled as starting <1 year prior to eruption but for others longer times are required for complete equilibration. This variety of times is most readily explained if the mixing occurred in a mush zone. None of the plagioclase phenocrysts from the Costa Rica Rift that we studied have Mg contents in equilibrium with their host basalt even at their rims, requiring mixing into a much more evolved magma within days of eruption. In combination these observations suggest that at both intermediate- and slow-spreading ridges: (1) the chemical environment to which crystals are exposed changes on annual to decadal time scales; (2) plagioclase crystals record the existence of melts unlike those erupted; and (3) disaggregation of crystal mush zones appears to precede eruption, providing an efficient mechanism by which evolved interstitial melt can be mixed into erupted basalts.

Keywords Plagioclase · Diffusion · MORB · Mixing

Communicated by T.L. Grove.

Electronic supplementary material The online version of this article (doi:10.1007/s00410-009-0432-3) contains supplementary material, which is available to authorized users.

F. Costa (✉)
Institut de Ciencies de la Terra 'Jaume Almera', CSIC,
08028 Barcelona, Spain
e-mail: fcosta@ija.csic.es

F. Costa · S. Chakraborty
Institut fuer Geologie, Mineralogie und Geophysik,
Ruhr-Universitat Bochum, 44780 Bochum, Germany
e-mail: Sumit.Chakraborty@rub.de

L. A. Coogan
School of Earth and Ocean Sciences, University of Victoria,
Victoria, BC V8W 3P6, Canada
e-mail: lacoogan@uvic.ca

Introduction

Approximately 20 km^3 of magma is processed through magma chambers along the global mid-ocean ridge system every year. Despite being the planet's largest volcanic system, little is known of the details of the magma plumbing system beneath ridges and how these vary with spreading rate. A key observation made by early researchers studying the petrology of mid-ocean ridge

basalts (MORB) is that phenocrysts are commonly not in equilibrium with their host suggesting magma mixing prior to eruption (e.g. Dungan and Rhodes 1978; Dungan et al. 1978; note that we use the term phenocryst to distinguish large crystals set in a fine grained matrix with no genetic connotation). However, despite having known that mixing is important in magma chambers at mid-ocean ridges for over 25 years our quantitative understanding of this process has not developed significantly. Here we return to this problem to investigate the time scales of magma mixing and magma–mush interaction beneath mid-ocean ridges.

Crustal residence times of magma, based on U–Th series disequilibrium data, have been calculated to be on the order of thousands of years (e.g. Goldstein et al. 1994). More recently, Rubin et al. (2005) used ^{210}Pb–^{226}Ra–^{230}Th radioactive disequilibria to infer that melts of the Earth's mantle can be transported, accumulated, and erupted in a few decades. Alternatively, Saal and Van Orman (2004), Van Orman et al. (2006), and Van Orman and Saal (2007) suggest that diffusive interaction between basalts and shallow level plagioclase-bearing gabbros may play a major role in generating U-series disequilibria providing an alternative explanation for these time scales.

Here we investigate the major and trace element zoning of plagioclase crystals in MORB to place better constraints on the times scales of magma mixing beneath mid-ocean ridges. This approach is based on modelling the diffusive re-equilibration of phenocrysts with the magma surrounding them. Two suites of samples are investigated, one from the slow-spreading Mid-Atlantic Ridge and the other from the intermediate-spreading rate Costa Rica Rift. We model the behaviour of Mg and Sr for three reasons. The diffusion coefficients and plagioclase-melt partition coefficient for these elements are well known, they diffuse at sufficiently different rates that they provide constraints on processes that occur on different time scales, and they diffuse rapidly enough to show measurable changes in concentration on year to decade time scales.

Geological background and previous work

Ocean Drilling Program Leg 106, Hole 648B, Mid-Atlantic Ridge

The first sample suite we have studied is from Ocean Drilling Program (ODP) Hole 648B on the summit plateau of the Serocki volcano, a small volcanic edifice in the axial summit graben on the Mid-Atlantic Ridge (MAR) just south of the Kane fracture zone (22°55′ N). We have investigated 3 samples from this drill core, two from the upper section and one from deeper levels (samples [106-648B-1R-2, 60-61], [106-648B-4R-1, 18-20], and [109-648B-16R-1, 32-34], hereafter referred to as [61], [18], and [32], respectively). These likely come from two different flows: 61 and 18 from one, and 32 from another (Shipboard Scientific Party 1988). The major element composition of bulk-rocks and glasses from this core are similar within error of analytical measurement and very uniform, with SiO_2 ~49 wt%, Al_2O_3 ~16 wt%, FeO* (FeO* = total iron as Fe^{2+}) ~9.8 wt%, MgO ~7.6 wt%, CaO ~11 wt%, Na_2O ~2.8 wt%, CaO/Na_2O ~3.9 wt% (Shipboard Scientific Party 1988). The observation that bulk-rock and glass major element compositions are so similar allows us to use the bulk-rock composition to gain reliable information about the equilibrium relations of the magma by minimisation of free energy (e.g. MELTS; Ghiorso and Sack 1995) or phase equilibria experiments. The trace element compositions (in particular 'high' Sr, Zr, Y, and Rb) suggest that these basalts are transitional between enriched and normal MORBs (Shipboard Scientific Party 1988). Meyer and Shibata (1990) studied the major and trace element zoning of some plagioclase crystals from this site. They found a variety of complex forms of zoning and proposed that the cores of these phenocrysts were not in equilibrium with the host basalt.

Grove et al. (1990) performed phase equilibria experiments on a basalt from the Serocki volcano. They concluded that the high anorthite content of many plagioclase crystals could not have crystallised from the host lava. Instead, they suggested that the plagioclase probably represent crystal accumulations from a more primitive melt or that they are left over from mixing between a plagioclase-phyric primitive magma and a more differentiated magma.

Ocean Drilling Program Leg 148, Hole 896A, Costa Rica Rift

ODP Hole 896A was drilled into 5.9-Myr-old oceanic crust that formed at the intermediate spreading rate Costa Rica Rift (spreading rate 3.6 cm/year to the south and 3.0 cm/year to the north) 1 km southeast of ODP Hole 504B. Three samples have been investigated from different depths in the drill core and are from different lava flows. One (148-896A-4R-1, 68-70) is from 220 mbsf, another (148-896A-14R-3, 21-24) from about 315 mbsf, and the deepest (148-896A-30R-1, 5-8) is from the bottom of the hole at about 460 mbsf. Hereafter, we will refer to these samples by the first part of the last numbers of their labels, that is 68, 21, and 5, respectively. The bulk-rock composition (Brewer et al. 1996) of basalts at these depths is SiO_2 49–50 wt%, Al_2O_3 15–17 wt%, FeO* 9–10 wt%, MgO 7.5–9.4 wt%, CaO 13.0 wt%, Na_2O 1.7–1.9 wt%, and CaO/Na_2O = 7.6–6.8 wt%. Analyses of glasses from the same depths as these samples do not exist but those within a few centimetres have similar compositions to the

corresponding bulk-rock (Fisk et al. 1996). The glass and bulk-rock compositions are in general more primitive (higher MgO and Ca/Na) than those from the Serocki volcano and overlap with primitive MORBs compiled by Presnall and Hoover (1987). Bulk-rocks have low concentrations of Zr (39–45 ppm), Y (20–24 ppm), and Sr (61–65 ppm), indicating that these are incompatible-element depleted MORB.

McNeill and Danyushevsky (1996) studied the compositions of glass inclusions in plagioclase and olivine and obtained homogenisation temperatures of 1,195–1,215°C. The compositions of the glass inclusions in high-Ca plagioclase are in general basaltic, but many have MgO > 10 wt%. McNeill and Danyushevsky (1996) considered these high-MgO inclusions to be affected by post-entrapment crystallisation and, when they corrected them for this effect, they obtained almost the same composition as the interstitial glasses except for higher CaO/Na_2O wt% of the inclusions. As shown below based on plagioclase MgO contents, high-MgO melts were involved in the genesis of these lavas and thus some of the high-MgO inclusions might be from widespread magmatic liquids. McNeill and Danyushevsky (1996) also reported Fo_{92} [Fo = 100*Mg/(Mg + Fe*), in mol] olivine in these samples consistent with the involvement of a very MgO-rich melt in their petrogenesis.

Analytical techniques

Laser ablation inductively coupled mass spectrometry (LA-ICP-MS)

Strontium abundances were determined using laser ablation ICP-MS at the University of Victoria using a New Wave 213 nm Nd-YAG UV laser and a Thermo X-series ICP-MS; 30 s of gas blank analysis was followed by 10–20 s of sample analysis. The laser power was ~0.8 mJ and the laser pulse frequency was 10 Hz. These conditions were used to minimise the spot size whilst ablating sufficient material for precise analysis. The analyses were calibrated against NIST 611, 613, and 615 using CaO as the internal standard (assumed to contain 497, 76, and 42 ppm of Sr and 11.5, 11.9, and 11.8 wt% of CaO, respectively, based on Pearce et al. 1997, and Horn et al. 1997). The gas blank was removed from all analyses and drift was corrected for by analysis of these standards before and after each sample. Precision, based on the relative standard deviation of 12 analyses of each glass standard, was better than 3%. Preliminary experiments to determine the relative efficiencies of glass and plagioclase ablation under these conditions suggest that calibration against NIST glass may introduce over-estimates of the Sr-content of the plagioclase of <10%. Absolute concentrations were determined using plagioclase CaO contents obtained from electron microprobe analyses prior to the LA-ICP-MS. Where the LA-ICP-MS analyses do not overlap with the electron microprobe traverses, their positions were projected on them.

Electron microprobe analyses

Plagioclase was analysed using an electron microprobe (SX-50 Cameca instrument at Ruhr-Universitat Bochum). The accelerating voltage was 15 kV and beam current was 30 nA. Counting times were 20 s for Al, Si, Ca, Na, Fe, K, and 60 s for Mg on the peak and half the peak time on each of the two background measurements. Spot size was ~2 μm diameter, and spacing between analyses varied between 4 and 5 μm.

Modelling parameters and method of calculation of melts in equilibrium with plagioclase

In the following sections we compare the measured plagioclase Mg and Sr contents with a series of modelled compositions calculated assuming either an equilibrium distribution of these elements, or that their distribution was controlled by diffusive loss or gain of the element from the crystal rims. The input parameters required for these models are described here and the modelling results are discussed in detail in later sections.

The concentrations of Mg and Sr in melts in equilibrium with plagioclase were calculated using the equations for plagioclase/silicate liquid partition coefficients (K_d) of Bindeman et al. (1998), and Blundy and Wood (1991). These K_d were used because they take into account the temperature and crystal composition which, since the liquid composition does not change dramatically, are the most important controls on the partition coefficient. The errors associated with the regression parameters that are used to obtain the partition coefficient are ~8–10% for Mg, and 5–7% for Sr (1σ).

We have used a temperature of 1,200°C for partitioning and diffusion calculations for both sample suites based on the equilibration temperatures discussed in previous sections. The partition coefficient for Sr has a small temperature dependence: a change of 50°C (at 1,200°C and for An_{80}) varies the partition coefficient by about 2.5%, whereas for Mg the change is ~10%. The K_d of both elements (and many others; Bindeman et al. 1998) increases with decreasing An content and thus crystals in intra-crystalline equilibrium have higher Mg and Sr contents in lower An zones. This gives a mirror image pattern between the trace elements and the An content that can be

used as a first order inference about the degree of equilibration of a given crystal.

The equilibrium distribution of MgO and Sr within plagioclase crystals is obtained following Costa et al. (2003): (1) we calculate the partition coefficients using the anorthite content and the equations of Blundy and Wood (1991) and Bindeman et al. (1998) at 1,200°C, (2) with the partition coefficients and the measured trace element concentration at the rim of the crystal we calculate a liquid composition in equilibrium with the rim. Care was taken to avoid the outermost rims with extremely high Mg concentrations (see below) since they are probably the result of fast growth and non-equilibrium partitioning (e.g. Albarede and Bottinga 1972). (3) Finally, the composition of the entire plagioclase crystal in equilibrium with the calculated liquid (and crystal rim) is obtained using the K_d for each portion of the crystal.

Petrological observations and plagioclase zoning profiles

Plagioclase zoning profiles in samples from ODP Hole 648B

The basalts studied from ODP Hole 648B are porphyritic with relatively large phenocrysts of plagioclase (up to 0.4 cm in longest dimension) or glomerocrysts (up to 0.6 cm in longest dimension) of plagioclase, sometimes olivine, and very rarely clinopyroxene. The phenocryst abundance is <10 vol% (measured using image analysis of the entire thin section) and is dominated by plagioclase. Phenocrysts are set in a fine-grained groundmass of mainly thin laths of plagioclase and clinopyroxene, and Fe–Ti oxides (for a more detailed petrographic description see Shipboard Scientific Party 1988).

A total of 16 plagioclase phenocrysts were analysed in detail for their core-to-rim, or rim-to-rim compositional variations by electron microprobe (23 traverses totalling ~2,200 analyses; Electronic Appendix). Most crystals show normal zoning patterns of decreasing anorthite content (anorthite = An = 100Ca/[Ca + Na], in mol) towards the rim (Fig. 1 and Electronic Appendix). They commonly have a homogenous subrounded core of ~An_{85}, or display irregular variations between $An_{88–75}$. Cores are in some cases surrounded by an intermediate zone of $An_{80–70}$ before reaching a rim of $An_{60–55}$. The high-An cores are always larger (100–800 μm) than the intermediate zones (20–250 μm) or the outermost rims (<50 μm). A few crystals have cores with lower An content (70–78 mol%) which in some cases are surrounded by an intermediate zone of higher An (An_{85}) followed by a rim that is normally zoned from $An_{69–62}$. These are almost identical to crystals 4 (herein MS_4) and 8 of Meyer and Shibata (1990; their Figs. 5 and 6; our Fig. 2). Plagioclase MgO concentrations vary between ~0.15 and 0.30 wt% and tend to be higher in crystal rims than cores (Fig. 1). In many crystals the An and MgO contents vary antithetically, like a mirror image consistent with close approach to intra-crystalline equilibrium. That said, crystal cores from the same sample can have different Mg but the same anorthite content indicating disequilibrium between crystals within the population (i.e. inter-crystalline disequilibrium). Some very high Mg concentrations occur right at the albite-rich rims (e.g. zones of <20 μm with up to ~0.45 wt% MgO) and are the result of very late, and extremely fast, non-equilibrium plagioclase growth (e.g. Kuo and Kirkpatrick 1982; Meyer and Shibata 1990), and they will not be considered any further. LA-ICP-MS analyses of three representative crystals with a clear core and a rim overgrowth, show Sr concentrations that vary between ~160 and ~220 ppm (Table 1). Unlike for Mg, there is no clear correlation between the Sr and anorthite contents; rims can have the same or lower Sr content than cores (Fig. 1).

The compositional and textural study of Meyer and Shibata (1990) of plagioclase from the same drill core reports similar finding to ours, with anorthite contents of An_{85-64}, and MgO = 0.15–0.25 wt% (note that we do not consider the secondary ion mass spectrometry (SIMS) Sr data presented by Meyer and Shibata (1990) to be reliable because their calibration did not pass through the origin on a plot of intensity ratio versus concentration. Since their lowest Sr content standard contains >2× the Sr of the unknowns this could cause major uncertainty in these data. The same is not true for their SIMS MgO contents, which they also note agree with electron microprobe data, and thus we do incorporate these data into our study).

We also analysed the composition of 8 olivines. Their forsterite content ranges between Fo_{77} and Fo_{84}, although within a given sample the maximum variation is <2% Fo. A couple of core-to-rim electron microprobe traverses showed that the crystals are virtually unzoned with only a slight decrease in the Fo content over the outermost 10 μm.

The types of An zoning patterns of this hole were also found by other authors at other sites on the MAR including basalts from DSDP Sites 395 and 396 which are very close to Hole 648B (e.g. Dungan and Rhodes 1978; Sato et al. 1979; Kuo and Kirkpatrick 1982) and basalts from DSDP Sites 333–335 about 1,600 km north of the 648B site (Flower et al. 1977; Donaldson and Brown 1977). In some cases even the details of the zoning are the same (e.g. reversely zoned patterns) and it is likely that the inferences that we derive apply more generally to MAR basaltic magmatic systems.

The subrounded cores of many plagioclase crystals, and the presence of reversals in An content from core-to-rim,

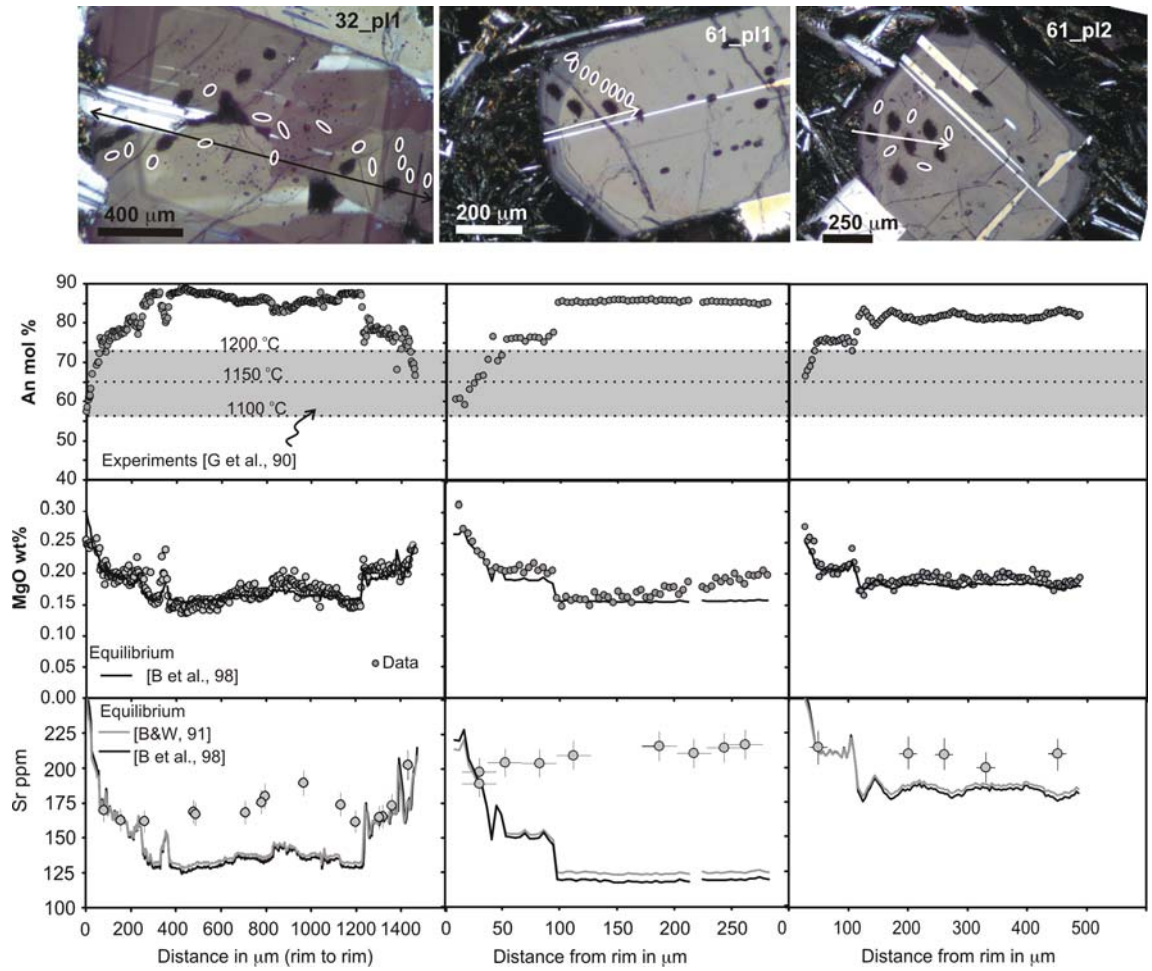

Fig. 1 Plagioclase photomicrographs and chemical zoning profiles of selected crystals from ODP Hole 648B (see labels at *top*). The *arrows* indicate the position of the electron microprobe traverse and the *white ellipses* the location of the pits from LA-ICP-MS analyses. The *grey band* on the anorthite content indicates the compositions of crystals from melting experiments of Grove et al. (1990) on basalts of the same ODP Hole. The *black* and *grey lines* in the MgO and Sr concentrations are the calculated composition of the crystals in equilibrium (at 1,200°C) with the crystal rim using the plagioclase/melt partitioning data from the references noted on the figure (see text for further details). [B et al. 98] = Bindeman et al. (1998); [B&W 91] = Blundy and Wood (1991). Note that the plagioclase MgO concentrations appear to be much closer to being in equilibrium with the crystal rims compared to the Sr contents which is consistent with the faster diffusion rates of Mg and hence more rapid internal equilibration

indicate that the plagioclase formed in an open system (e.g. Dungan and Rhodes 1978; Kuo and Kirkpatrick 1982; Meyer and Shibata 1990). The results of phase equilibria experiments (Grove et al. 1990) on basalts from this site show that plagioclase An_{73} and olivine Fo_{84} co-crystallise at 1,205°C close to the ~0.1 MPa liquidus. The An and Fo content of plagioclase and olivine, decrease from 73 to 56, and from 84 to 65, respectively, with decreasing temperature from 1,205 to 1,108°C at the quartz–magnetite–fayalite (QMF) oxygen fugacity buffer. Most of the plagioclase core compositions from the natural rocks of An_{85} to An_{78} were not experimentally reproduced indicating that at least parts of the crystals likely grew from a more primitive and/or more depleted (higher Ca/Na) melt (Grove et al. 1990; Fig. 1). In contrast, the plagioclase composition of the inner rims (ca. $An_{73–75}$) and the olivine forsterite content are reproduced at $1{,}205 < T < 1{,}174$°C. This range of temperature is close to the liquidus temperature of 1,209°C calculated using MELTS (Ghiorso and Sack 1995) at dry conditions, QMF oxygen buffer, and ~0.1 MPa. In these calculations the liquidus phase is plagioclase (An_{72}) and olivine (Fo_{81}) appears at 1,190°C. Increasing the pressure of equilibration in these MELTS model decreases the anorthite content of the first plagioclase to crystallise down to An_{38} at 1.5 GPa, and this mineral disappears between 1.5 and 2 GPa. Adding 0.5 to 1 wt% water to the bulk-composition increases the An content of the plagioclase by about 5 mol% at total pressures between 0.1 and 0.5 GPa. This indicates that the high-An (e.g. >80) cores of many crystals grew from melts of higher Ca/Na than the host rock and probably also at shallow depths.

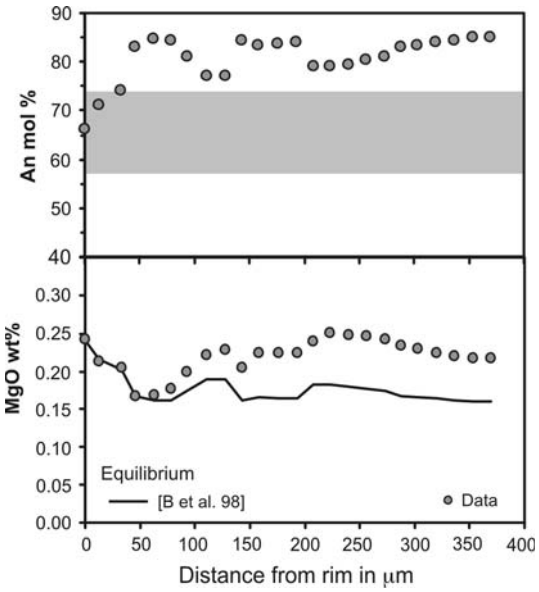

Fig. 2 Zoning of plagioclase crystal 4 from Meyer and Shibata (1990). The *grey band* on the anorthite content indicates the compositions of crystals from equilibrium experiments of Grove et al. (1990) on basalts of the same ODP Hole. The *black line* on the figure shows the MgO concentrations is the calculated MgO zoning assuming equilibrium (at 1,200°C) with the crystal rim (see text for further details). See Meyer and Shibata (1990) for photomicrograph and additional information

Plagioclase zoning profiles in samples from ODP Hole 896A

The basalts from ODP Hole 896A are petrographically similar to those from ODP Hole 648B. Plagioclase (up to 0.25 cm in longest dimension) is the most abundant phenocryst and it is found as isolated grains and, more rarely, in glomerocrysts with other plagioclase and/or olivine (and in one case with Cr-spinel). Rare clinopyroxene occur as isolated crystals. The total phenocryst content in the studied samples is also low (<10 vol%) and the groundmass is microcrystalline and contains mainly thin laths of plagioclase and small clinopyroxene. For more details about the petrography see Alt et al. (1993).

A total of 13 crystals from 3 samples were investigated in detail with the electron microprobe (14 traverses with 4–5 μm spacing and about 1,200 total analyses; Electronic Appendix). Plagioclase cores are either homogeneous or show minor compositional variations (Fig. 3 and Electronic Appendix), with An ranging from 75 to 88, but the majority are between An_{80} and An_{85}. Except for one crystal, which shows a progressive decrease in anorthite content from the core (An_{80}) to the rim (An_{55}), most plagioclase crystals change abruptly to lower An contents ($An_{70–60}$) within ~20 μm of the margins. Dissolution features occur within the core, or at the core-to-rim

Table 1 Anorthite (mol%; electron microprobe) and Sr (ppm; LA-ICP-MS) contents of plagioclase traverses

Analysis label	Distance from rim (μm)	An	Sr
648-b32-pl1-8	80	74.4	170
648-b32-pl1-9	150	78.3	162
648-b32-pl1-10	260	86.7	162
648-b32-pl1-11	480	88.6	169
648-b32-pl1-12	490	88.6	167
648-b32-pl1-7	710	87.2	168
648-b32-pl1-13	780	84.2	175
648-b32-pl1-6	790	84.2	180
648-b32-pl1-5	970	87.2	189
648-b32-pl1-14	1130	87.2	174
648-b32-pl1-4	1190	88.2	161
648-b32-pl1-15	1300	79.3	165
648-b32-pl1-2	1310	78.4	165
648-b32-pl1-1	1350	76.9	173
648-b32-pl1-3	1420	73.4	202
648-b-61-pl2-4	50	75.4	215
648-b-61-pl2-2	200	82.3	210
648-b-61-pl2-3	260	83.3	209
648-b-61-pl2-1	330	81.8	200
648-b-61-pl2-5	450	83.3	210
648-b61-pl1-6	30	68.1	198
648-b61-pl1-7	30	68.1	189
648-b61-pl1-11	50	73.5	205
648-b61-pl1-12	80	86.4	204
648-b61-pl1-13	110	86.4	210
648-b61-pl1-15	190	86.4	217
648-b61-pl1-10	240	86.4	216
648-b61-pl1-14	220	86.4	211
648-b61-pl1-9	260	86.4	218
896-68-pl1-2	40	82.1	86
896-68-pl1-3	70	81.9	105
896-68-pl1-4	90	78.4	115
896-68-pl1-5	110	76.7	120
896-68-pl1-9	110	76.8	117
896-68-pl1-6	130	76.7	115
896-68-pl1-7	150	76.8	118
896-68-pl1-8	160	78.9	114
896-21-pl1-1	40	86.7	75
896-21-pl1-11	50	88.2	76
896-21-pl1-2	75	86.7	79
896-21-pl1-10	100	86.2	78
896-21-pl1-8	130	88.2	85
896-21-pl1-4	200	86.7	92
896-21-pl1-7	260	86.2	93
896-21-pl1-6	330	86.7	92
896-21-pl1-5	400	86.7	96

transition, but others have euhedral cores. The MgO content of the plagioclase cores varies from 0.17 to 0.3 wt%. Abrupt increases up to 0.45 wt% MgO right at the crystal rims probably reflect disequilibrium partitioning during rapid growth. As with the Hole 648B phenocrysts, plagioclase MgO concentrations tend to be a mirror image of the An zoning patterns, with high-An content correlated with low MgO and vice versa (Fig. 3). Sr concentrations of two crystals vary between ~75 and ~125 ppm (Table 1). Core-to-rim traverses show approximately constant Sr contents in the cores with decreasing Sr in the rims. Crystals within the same thin section, and with identical An content, can have different Mg contents which shows that there is some inter-crystal disequilibrium and that the crystals equilibrated with slightly different melts.

The zoning patterns of these plagioclases are less varied than those of plagioclase from ODP Hole 648B; for example, we have not found reversals of An content larger than 10% in any of the profiles. We have obtained liquidus temperatures of 1,233°C using the measured bulk-composition of these basalts at dry conditions, on the QFM oxygen buffer, and 0.1 MPa using the MELTS algorithm (Ghiorso and Sack 1995). At ~1,210°C plagioclase at An_{84} and olivine at Fo_{84} coexist with clinopyroxene and thus, the plagioclase phenocryst An content appears to be in equilibrium with the host rock at about this temperature. A similar temperature of equilibration (between 1,195 and 1,215°C) was determined by McNeill and Danyushevsky (1996) from homogenisation of glass inclusions in plagioclase. However, these authors also report more Ca-rich

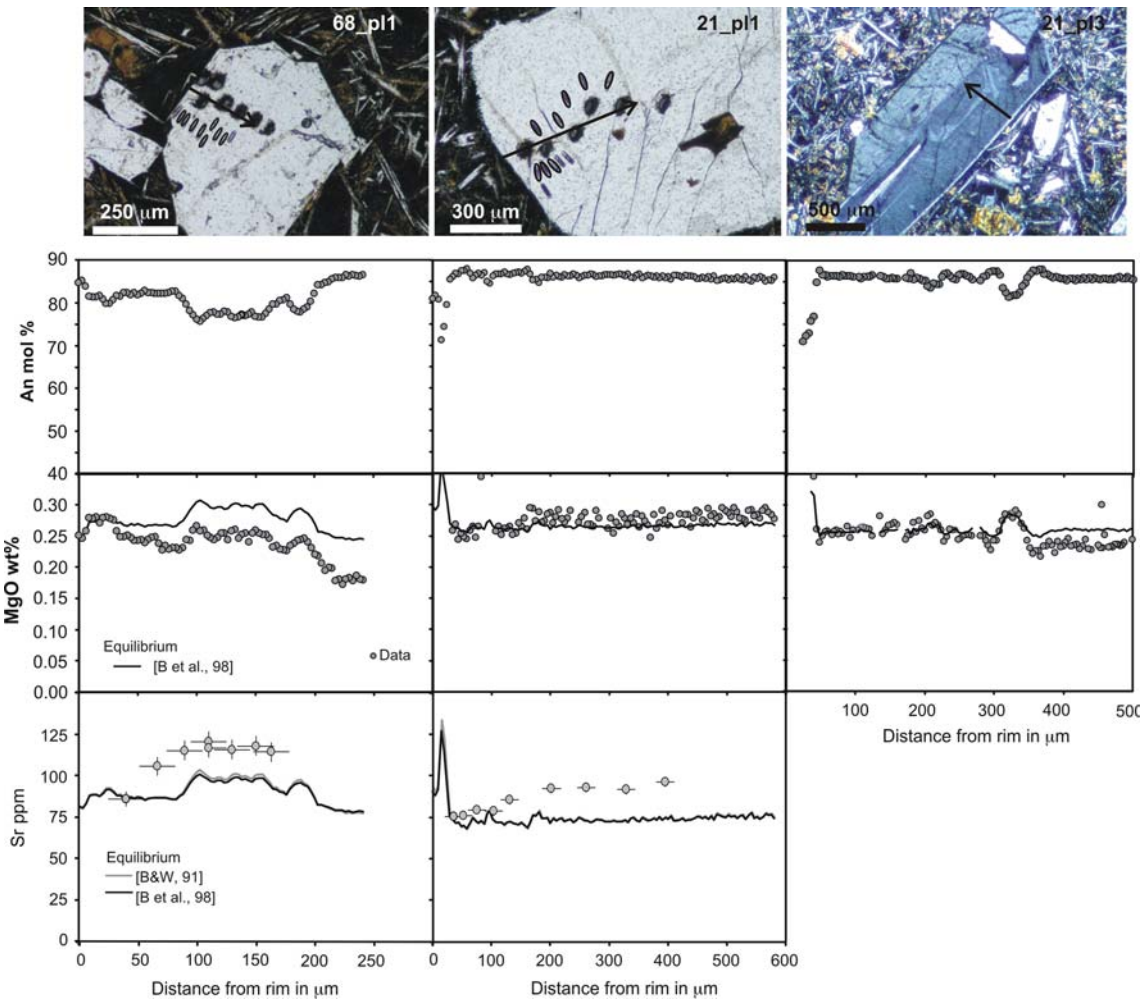

Fig. 3 Plagioclase photomicrographs and chemical zoning profiles of selected crystals from ODP Hole 896A. The *arrows* indicate the position of the electron microprobe traverse and the *black ellipses* the location of the pits from LA-ICP-MS analyses. The *black* and *grey lines* in the MgO and Sr concentrations are the calculated composition of the crystals in equilibrium (at 1,200°C) with the crystal rims calculated using the plagioclase/melt partitioning data from the references notes in the figure (see text for further details). [B et al. 98] = Bindeman et al. (1998); [B&W, 91] = Blundy and Wood (1991). Note that the plagioclase MgO concentrations appear to be much closer to being in equilibrium with the crystal rims compared to the Sr contents which is consistent with the faster diffusion rates of Mg and hence more rapid internal equilibration

plagioclase (up to An_{94}) and more Mg-rich olivines (up to Fo_{92}) from this site. Such high values of An and Fo cannot be in equilibrium with the host at any pressure, temperature, and H_2O content (based on a series of MELTS calculations) and indicate that more primitive and/or depleted magmas (higher Ca/Na and Mg/Fe) were involved in the evolution of these basalts. An open system history is also indicated by the over-enrichment in large crystals in crystal size distribution patterns (Alt et al. 1993) and, as discussed below, by the calculated liquid compositions.

Calculated melt Sr and MgO concentrations in equilibrium with plagioclase and petrogenetic models

The evidence of open system magmatic processes gathered from the types of major element zoning and absolute An contents discussed in the previous section are refined here using the MgO and Sr concentrations. We first address the issue of whether these elements are equilibrated within the crystals by diffusion. Note that homogenisation of the anorthite content by diffusion takes unrealistically long times even at magmatic temperatures due to the slow NaSi–CaAl diffusion (Grove et al. 1984), whereas Sr is about 4 orders of magnitude faster, and Mg (LaTourrette and Wasserburg 1998) is about 60 times faster than Sr (Gilleti and Casserly 1994; comparison at An_{80} and 1,200°C). In a second step we calculate the liquids in equilibrium with the plagioclase crystals and compare these to the host-rocks compositions. Then we describe a qualitative model to explain these data. In the last section before the "Discussion" we derive time constrains for the magmatic processes using a diffusion model.

Samples from ODP Hole 648B

Plagioclase An and MgO content vary antithetically in many crystals or parts of crystals (Fig. 1) with cores generally having high An and low MgO compared to rims. This MgO distribution is the opposite of what would be expected from differentiation, where fractionation of olivine and plagioclase would produce more differentiated melts with lower Ca/Na and lower MgO concentration (e.g. Grove et al. 1992). The measured MgO concentrations and the profile shapes of all but two crystals overlap with those calculated to be in equilibrium with melt in equilibrium with the crystal rim (Fig. 1). According to our interpretation, this suggests that the initial (growth) zoning of Mg has been destroyed by re-equilibration via diffusion. One of the exceptions is the core of crystal 61_pl1 in which the measured MgO concentration decreases, but the An content stays constant, and thus the MgO profile should also be homogenous within the core at equilibrium (Fig. 1). The other is crystal MS_4 (Meyer and Shibata 1990) that also has MgO contents of cores and rims that are not in equilibrium (Fig. 2). These two crystals, which both come from the upper flow sampled at this drill site, can thus provide information about the time scales of magmatic process beneath the Serocki volcano (see sections below). Notably, these are not the largest crystals analysed; lack of evidence for disequilibrium in larger crystals, which should take longer to diffusively equilibrate, indicates that different crystals have different histories.

The majority of liquids calculated to be in equilibrium with plagioclase contain between 8 and 9 wt% MgO (Figs. 4 and 5) and overlap with, or are slightly more MgO-rich than, the whole-rock MgO contents. Thus, most plagioclase phenocrysts can be considered to be close to equilibrium with respect to MgO of their host rock. The two crystals that show disequilibrium MgO distributions have cores in equilibrium with more MgO-rich melts. Melts in equilibrium with different portions of crystal 61_pl1 have MgO contents that decreases from ~10 to 8 wt% mainly in its core (Fig. 4); for crystal MS_4 the calculated melt MgO content decreases from ~11 to 8 wt% from core to rim (Fig. 5).

The Sr content of plagioclase shows no simple relationship with the anorthite content of the plagioclase indicating that the crystals are not in internal equilibrium. The Sr concentration of a melt in equilibrium with the cores of the plagioclase crystals is ~150 ppm, overlapping with the Sr content of the host-rock (Fig. 4; Shipboard Scientific Party 1988). As the abundance of phenocrysts is low, the bulk-rock Sr content must be very similar to the melt Sr content. The rims of crystals 32_pl1 and 61_pl1 are in equilibrium with a melt with much lower Sr contents of ~100 ppm (Fig. 4). This means that the rims of crystals 32_pl1 and 61_pl1 were not in equilibrium with the Sr content of the melt in which they were transported to the surface, whereas the whole of crystal 61_pl2 was close to equilibrium with this melt. The observation that the rims of two crystals, which come from different flows, are not in equilibrium with their host but grew from or equilibrated with a melt with lower, but similar, Sr contents is quite surprising. This contrasts with the observation that the rims of plagioclase crystals are approximately in equilibrium with the melt they were erupted in both in terms of their An (e.g. Grove et al. 1990) and MgO contents.

Significant Sr depletion in the plagioclase rims could be explained by: (1) extensive crystallisation of a plagioclase-rich assemblage (bulk $K_d > 1$) producing a melt with low Sr from which these crystal rims grew or equilibrated; (2) invasion of the crystal mush by an incompatible element depleted (including Sr) melt; (3) rapid disequilibrium growth leading to a Sr-depleted boundary layer around the growing

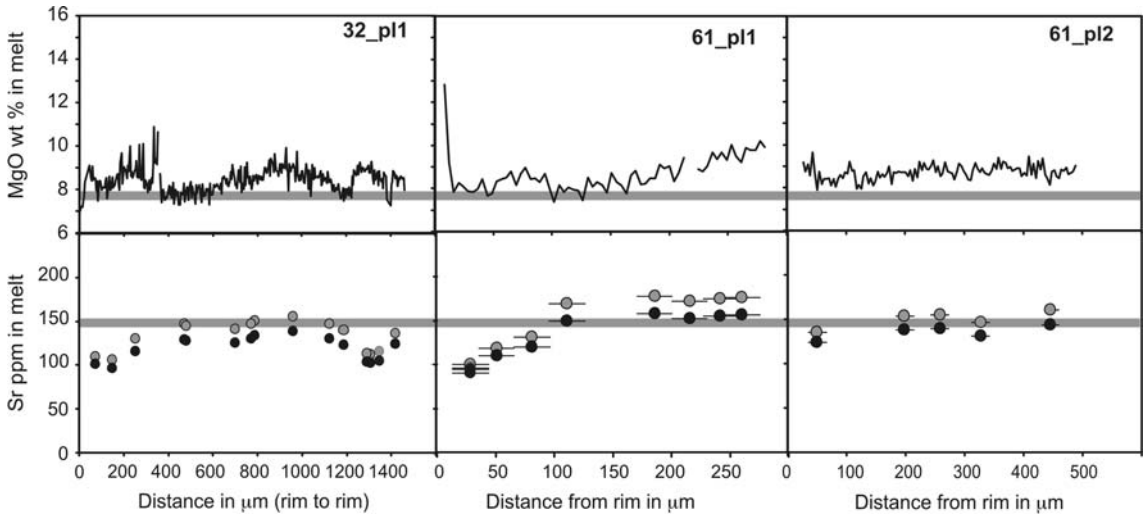

Fig. 4 Calculated MgO wt% and Sr ppm of liquids in equilibrium with plagioclase using plagioclase/melt partition coefficients. *Grey bands* delimit the compositions of the bulk rocks and interstitial glasses. The calculated MgO content of melts in equilibrium with the crystals overlaps, or is slightly higher than, those of the bulk-rocks. Note that for crystal b61_pl1 the innermost part of the crystal core records equilibrium with a melt with higher MgO than the outer core. This could be interpreted as reflecting the partial requilibration of the crystal from initially being in equilibrium with a high-MgO melt towards equilibrium with a lower MgO melt, such as the one that transported it to the surface. The calculated Sr concentrations of the plagioclase cores are more or less in equilibrium with the bulk rock compositions, whereas the rims of crystals 32_pl1 and 61_pl1 are in equilibrium with melts with lower Sr content, probably reflecting a closed system crystallisation event (see also text for more discussion)

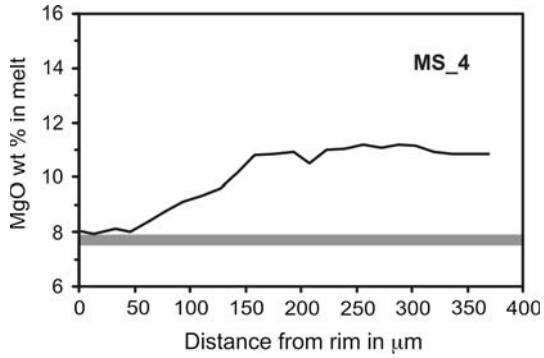

Fig. 5 Calculated MgO wt% of liquids in equilibrium with crystal MS_4 of Meyer and Shibata (1990). The *grey band* delimits the concentration of MgO in the bulk rocks and interstitial glasses from Site 648B. The core of the crystal is in equilibrium with a melt with a much higher MgO content than any erupted but the rim is close to equilibrium with the erupted melts. We interpret this in the same way as for crystal 61_pl1 shown in Fig. 4

crystals and hence Sr-poor plagioclase crystals; or (4) analytical artefacts or uncertainties in the partition coefficients. In the first model crystallisation of interstitial melt in a plagioclase-rich crystal mush would be required to drive the melt to low Sr contents because a decrease in melt mass of $\geq$50% is required to drive the Sr content down. In this case growth of the plagioclase rims from such an interstitial melt, or diffusive equilibration of initially more Sr-rich rims, could lead to the observed Sr-poor plagioclase rims; this seems to be the best explanation for these data. The possibility of having a Sr-poor melt arriving at the reservoir is an alternative explanation but if the Sr-poor plagioclase rims grew from an incompatible element depleted melt (model 2) they would be expected to be Na-poor (e.g. Klein and Langmuir 1987); instead the Sr-depleted plagioclase rims are Na-rich. The potential of rapid disequilibrium growth as an explanation for the Sr-poor plagioclase rims (model 3) can be tested by determining the growth rate necessary to reproduce the data. We have done this using an analytical solution to the equations that describe coupled growth and diffusion in the melt from Smith et al. (1955; their Eq. 10). Using a diffusion coefficient for Sr in the melt of 1×10^{-11} m^2 s^{-1} from Lesher (1994) and a partition coefficient of between 1.7 and 1.9 (for $An_{70–75}$), the Sr concentrations in the outer $\sim$100 μm of the crystal can be fit using a growth rate of $\sim$1–5 $\times$ 10^{-6} cm s^{-1}. These growth rates are about 3 orders of magnitude higher than those determined for natural plagioclase in mafic liquids (Cashman 1990, 1993; Hammer 2008) and seem unrealistic. Uncertainties in both the data and partition coefficient are too small to explain the large variations in Sr content in these crystals.

While numerous possible models could explain the data the simplest model is as follows. An open system magma chamber crystallised primitive plagioclase ($\sim An_{85}$) and olivine from melts that contained up to at least $\sim$11 wt% MgO. Replenishment events caused resorption of plagioclase and in some cases led to increasing An contents at the rims of the growing plagioclase crystals (observed now as the high-An intermediate zones). Crystals accumulated to form a crystal mush zone in which continued crystallisation

led to differentiation of the interstitial melt. The interstitial melt generally evolved to lower Ca/Na, MgO, and Sr explaining the low An, low Sr plagioclase rims but the extent of differentiation was locally variable. For example, in regions with high olivine contents the interstitial melt was buffered to higher MgO contents. Mush zones are probably heterogeneous judging from studies of oceanic gabbros that are interpreted to form from solidifying these zones (Perk et al. 2007). These include high-Mg troctolites in places in which the interstitial melt MgO must have been buffered to high values prior to solidification. This means that diffusive exchange of MgO between plagioclase crystals and the interstitial melt led to plagioclase with different MgO contents in different parts of the mush; generally though plagioclase crystals equilibrated with an interstitial melt much less Mg-rich than the one from which they initially crystallised. Finally, this crystal mush was disrupted by, and crystals from it entrained into, a replenishing melt. This melt would have mixed with interstitial melt and any overlying magma to produce the magma erupted. Therefore, depletion of Sr in a melt reservoir of limited mass (the interstitial melt) appears to be the best explanation for this observation.

Samples from ODP Hole 896A

As with the samples from ODP Hole 648B most plagioclase crystals in samples from Hole 896A have MgO distributions that vary broadly antithetically with the An content, although one crystal shows clear intra-crystal disequilibrium (Fig. 3) and others show less extreme disequilibrium. The calculated melt MgO concentrations in equilibrium with the plagioclase in samples from Hole 896A range from 9 to 15 wt%, with the majority between 12 and 13 wt% (Fig. 6). These MgO concentrations partly overlap with, but are typically higher than, the MgO content of the bulk-rocks, interstitial glasses, or recalculated glass inclusions (McNeill and Danyushevsky 1996), which vary between 7.5 and 9.5 wt%. These high-MgO contents are not due to kinetics of fast growth because they occur throughout large crystals (>500 μm). It is possible that parts of the crystals did grow at fast rates and incorporated Mg at disequilibrium concentrations (e.g. Albarede and Bottinga 1972) but such features would have been quickly erased by intra-crystalline diffusion of Mg (see below). Most crystals show rather homogenous MgO concentrations (Fig. 3b), but the compositions of liquids in equilibrium with other crystals increase from the core-to-rim, from ~9 or 11 to ~13 wt% MgO (Fig. 6a–c). The melts in equilibrium with the plagioclase rims all contain ~13 wt% MgO indicating that the crystals equilibrated with a similar primitive liquid, despite being from different flows. It is unlikely that the plagioclase-melt partition coefficients (Bindeman et al. 1998) are in error because we have obtained reasonable results using them for plagioclase from ODP Hole 648B. Moreover, inappropriate partition coefficient of Mg cannot explain the increase in the MgO of the liquid calculated to be in equilibrium with the crystal from its core to rim (Fig. 6).

The high-MgO content of the melts calculated to be in equilibrium with plagioclase, and the decreasing MgO from rim to core, may be partially related to uncertainty in the temperature of equilibration. For example, if the crystals equilibrated with, or grew from, a more mafic melt than the host rock it probably had a higher temperature that the one that we have inferred (i.e. 1,200°C). If we use 1,250°C for the calculation we find that the crystals grew from, or equilibrated with, a liquid with ~11.5 wt% MgO (Fig. 6). This is still higher than any erupted MORBs, but is within the range that has been inferred for near primary MORB (e.g. Langmuir et al. 1992). We conclude that the high-MgO recorded in these plagioclase crystals reflects diffusive equilibration with a high-Mg melt, and this process is recorded in the crystals that show increasing Mg towards their rim.

McNeill and Danyushevsky (1996) analysed glass inclusions within plagioclase crystals from Hole 896A and found a large variation of MgO content, from about 8 up to 16 wt% MgO. They concluded that the high-MgO contents were the result of post-entrapment crystallisation, and that the most likely initial MgO was that of the host glass of about 9.5 wt% MgO. However, we have used their reported plagioclase compositions (their Table 3) that hosted the analysed glass inclusions and calculated that the MgO content of the equilibrium liquid at 1,250°C should be between 8 and 12 wt% (with a couple of analyses up to 16 wt%). Thus it seems that although the MgO of the inclusions might have been affected by post-entrapment crystallisation some of them could be samples of high-MgO liquids in contact with the crystals. The presence of Mg-rich olivine crystals (up to Fo_{92}) in this drill core (McNeill and Danyushevsky 1996) is consistent with the interpretation of plagioclase equilibration with Mg-rich magma.

Notwithstanding the details of the interpretation of the high-Mg in these plagioclases, it is clear that they did not equilibrate with the MgO content of the melt that transported them to the surface and we use this observation to obtain time scales for magma mixing and eruption in the next section. The calculated melt Sr concentrations in equilibrium with plagioclase vary from ~60 to 85 ppm (Fig. 6), partially overlapping with the basaltic bulk-rock from the same depth in the core (61–65 ppm), and fall within the maximum range for the entire drill core of 53–83 ppm. Because of this we make the conservative interpretation that the Sr content of these plagioclase are too close to the equilibrium concentration to provide reliable information about time scales of magmatic processes.

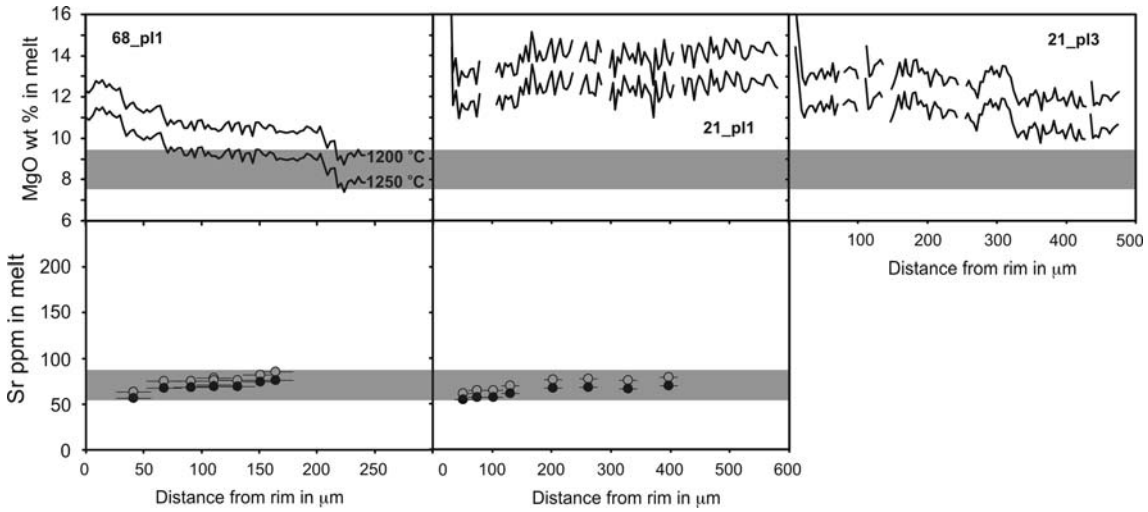

Fig. 6 Calculated MgO (wt%) and Sr (ppm) contents of liquids in equilibrium with plagioclase. The *grey bands* are the ranges of concentrations of the bulk rocks and interstitial glasses from the drill core. Note that the calculated MgO of the liquid in equilibrium with plagioclase is significantly higher than the bulk rock except for the core of one crystal (68_pl1), where the two almost overlap. Melt MgO contents calculated using the partition coefficients for two temperatures (1,200 and 1,250°C) are shown. The calculated Sr content of the melts in equilibrium with the plagioclase, calculated using the two different partition coefficients described in the text and Fig. 3 (at 1,200°C) are similar or slightly higher than the concentrations in the bulk-rocks

A relatively simple magma reservoir model can explain the petrogenesis of the Hole 896A samples. A primitive and depleted MORB containing 60–85 ppm Sr crystallised plagioclase ($An_{80–85}$) and olivine and the crystals accumulated forming a crystal mush. Even more primitive melt, containing ~11–13 wt% MgO, percolates through this mush and Mg diffuses into the plagioclase crystals. In most cases this processes started long enough before eruption that the plagioclase completely equilibrated with this melt prior to eruption but in rare cases (e.g. crystal 68_pl1) there was insufficient time for complete equilibration. Equilibration with this Mg-rich melt can explain the forsteritic olivine (Fo_{92}) in this drill core (McNeill and Danyushevsky 1996) and its high temperature can explain the lack of overgrowth of low An rims on the plagioclase crystals. Mixing within a crystal mush zone is supported by the different histories recorded by different crystals including: (1) different crystals in the same sample being in internal Mg equilibrium but not being in equilibrium with one another; and (2) the fact that the crystals that show internal Mg disequilibrium are not the largest crystals in the sample even though the largest crystals should take the longest to equilibrate. If the crystals recorded mixing in a melt-dominated reservoir similar histories would be expected for all of them. Immediately before eruption the crystal mush was disrupted and the crystals were mixed into the magma in which they were erupted. This occurred very shortly prior to eruption since the Mg content of the plagioclase rims has not reequilibrated with the host melt. This process must have happened repeatedly because the same history is recorded in samples from different flows. Below we put constraints on the time scales for these processes.

Diffusion modelling to extract the time scales of mixing processes recorded in plagioclase crystals

In this section we use diffusion models to evaluate the time scales of magmatic processes based on those crystals that show intra-crystal disequilibrium. Prior to obtaining the time scale information it is necessary to have a precise conceptual model for the magmatic processes involved in the petrogenesis of the basalts, and these have been schematically summarised in Fig. 7 based on the discussion in the previous section. The exact time scales of processes derived from modelling diffusion profiles in individual crystals only apply to those individual crystals but the overall picture that comes out is of repeated changes in the chemical environment of these crystals on annual to decadal time scales.

In the model for the petrogenesis of the Hole 648B samples outlined above the timescale of several processes can be determined by the extent of diffusive equilibration that has occurred. Plagioclase crystals with cores in equilibrium with melts more MgO-rich than their rims (61_pl1 and MS_4) can be explained by diffusive loss of MgO from crystal rims either within the mush zone or after entrainment into the melt in which they were erupted. Retention of disequilibrium between plagioclase rims and the melt in which they were erupted in terms of Sr provides a maximum time between the disruption of crystals from the

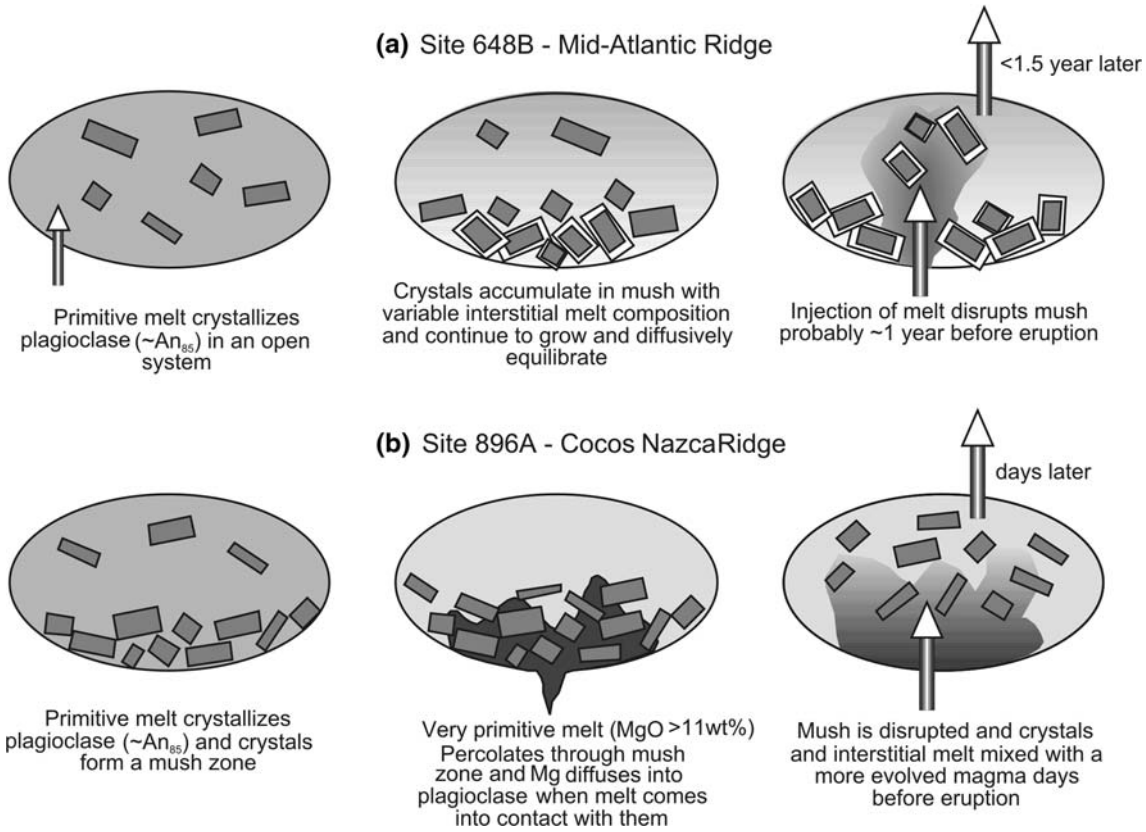

Fig. 7 Magma chamber models for **a** Site 648B and **b** Site 896A. **a** A primitive magma crystallised An-rich plagioclase (and olivine) in an open system reservoir where more than one mixing or mingling episode occurred. Eventually these crystals became part of a crystal mush zone. Continued crystallisation of interstitial melt led to the formation of lower An rims and depleted the Sr content of the interstitial melt. The MgO content of the interstitial melt (and plagioclase in the mush zone) was heterogeneous due to variable buffering by differing amounts of olivine. Later the mush was disaggregated and crystals and interstitial melt mixed into the erupted magma. **b** Plagioclase (and olivine) crystallised from a primitive melt and accumulated to form a mush zone. A very primitive melt migrated into this mush zone and Mg diffused into the plagioclase crystals. The mush zone was disrupted by a more evolved melt and eruption occurred within days. *Darker shading* represents more primitive compositions for both the melt and crystals

crystal mush and quenching on the seafloor. Disequilibrium of the Sr concentration between the rims and cores of the plagioclase crystals provides a maximum time that the crystals can have existed in the crystal mush zone.

For plagioclase crystals from Hole 896A that show internal MgO disequilibrium (e.g. 68_pl1; Fig. 3) the time interval between when the percolation of high-MgO magma into the crystal mush zone and eruption can be constrained. For other crystals that have equilibrated with the high-MgO melt, only the minimum time intervals can be established. Additionally, the maximum time between disaggregation of the crystal mush zone and quenching on the seafloor can be determined based on the preservation of MgO disequilibrium between the crystal rims and host basalt.

Approach to calculating time scales of magmatic processes

The observation that the MgO and Sr concentrations within several plagioclase crystals are not equilibrated can be used to determine the time interval between the different magma mixing events and the quenching of the basalts on the seafloor. For this we need estimates of the initial concentrations, the boundary conditions, a diffusion model, and diffusion coefficients of the elements of interest (e.g. Costa et al. 2003, 2008).

We use the Sr diffusion data of Giletti and Casserly (1994) but we note that the data of Cherniak and Watson (1994) overlaps with this and thus yield similar results within error. For Mg we have used Eq. 8 of Costa et al. (2003) for the dependence of the diffusion coefficient on the plagioclase An content, which is based on the data of LaTourrette and Wasserburg (1998). We have also used the diffusion model and Eq. 7 of Costa et al. (2003) that considers the effect of variable anorthite content on the equilibrium profile shapes and diffusion coefficients. For a plagioclase An_{80}, a change of temperature from 1,200 to 1,250°C increases the diffusion coefficients, D_{Sr} and D_{Mg}, by a factor of ~ 2, which translate directly to time scales/durations.

We have used those recorded in the core of the crystals as initial concentrations and those at the rims as the conditions of the boundary. We have used fixed concentrations at the rims as boundary conditions and constant crystal size and temperature in all modelling as the system is not well enough constrained to warrant varying these parameters.

Magma mixing time scales beneath the Serocki volcano (ODP Hole 648B)

The *maximum* time interval between the entrainment of plagioclase from the crystal mush into the magma in which they were erupted and quenching on the seafloor can be constrained from the time it would take to eradicate Sr disequilibrium between the melt and plagioclase crystal rims. This estimate depends on the distance of the analysis to the rim, which varies between 80 μm for crystal 32_pl1 and 30 μm for 61_pl1 leading to times between ~7 and ~1.5 years, respectively. We have not calculated a time for crystal 61_pl2 because it is already close to equilibrium with the bulk rock (Fig. 5).

Most plagioclase phenocrysts have MgO concentrations that are almost completely in equilibrium with the host rock or surrounding glass (e.g. Fig. 1) and do not provide information about the time scales of sub-ridge processes. The two exceptions are crystals 61_pl1 and MS_4 (Meyer and Shibata 1990). Modelling the MgO concentrations of these crystals (see caption of Fig. 8 for details about initial and equilibrium concentrations) gives time of about a year in both cases. This corresponds to the time between when the crystals were mixed with a lower MgO magma, most likely upon disruption of the crystal mush, and when eruption occurred. This time estimate is consistent with the estimate from the Sr distribution that this mixing occurred <1.5 years prior to eruption.

The time required to fully equilibrate the Mg contents of the other plagioclase crystals can be estimated assuming that they had the same initial composition as the two that are not fully equilibrated and that their MgO has been completely homogenised by diffusion. To do such a calculation we need to account for the effects of three dimensions and we have used the diffusion equations for a parallelepiped (e.g. Eqs. 14.33 and 14.14 of Crank 1975) and the mean composition of the anorthite to calculate the diffusion coefficient. We have assumed the third dimension to be of the same length as the shortest dimension of the crystal as seen in this section. This gives minimum times for Mg homogenisation of between about 1 and 10 years (e.g. 4 years for crystal 32_pl1, and 6 years for crystal 61_pl2). This homogenisation could have occurred either: (1) within the mush zone in regions, where the interstitial melt was less MgO-rich than that surrounding crystals 61_pl1 and MS_4, or (2) after disaggregation of the mush if this occurred at different times in different places. The former model seems more likely as the latter requires the fortuitous scenario that separation of crystal 32_pl1 occurred long enough before eruption to allow complete Mg homogenisation (>4 years) but not long enough before eruption to allow the outermost analysed spot to reach Sr equilibrium with the new melt (<7 years).

The *maximum* time that the plagioclase crystals could have resided within the crystal mush prior to eruption (at high magmatic temperature) can be determined by assuming that the entire plagioclase grew from a melt with 150 ppm Sr and then was brought into contact with a melt containing 100 ppm Sr and the observed Sr profile was produced by diffusion after this. More likely the rim grew from a melt with progressively decreasing Sr content and thus the residence time of the crystals in the mush must have been shorter. The maximum mush residence times for plagioclase 32_pl1 and 61_pl1, are 140 and 7 years, respectively. As discussed above, the observation that plagioclase sometimes have subrounded cores, and intermediate zones of higher An content than their cores, points to magma mixing even earlier in the crystals' history. However, our data do not provide information about the timing of these events.

Magma mixing time scales beneath the Costa Rica Rift (ODP Hole 896A)

The rims of plagioclase crystals from Hole 896A have MgO concentrations in equilibrium with a melt that is more MgO-rich than their host rocks. This allows us to determine the *maximum* time interval between mixing these crystals into their host melt and eruption. Using the same approach as described above we obtain a time of <10 days; i.e. magma mixing occurred immediately prior to eruption.

A few plagioclase crystals show internal MgO disequilibria, but only in crystal 68_pl1 is the zoning pronounced enough that it can be used to constrain a detailed diffusion model. The Mg distribution of this crystal records the mixing event that led to the high Mg in these plagioclase crystals with the crystal rim, but not core, in equilibrium with the high-MgO melt. The rest of the crystals largely equilibrated with the same liquid (e.g. Fig. 7) and a 3D model for requilibration of the Mg in the same manner as for the crystals from Hole 648B gives similar times from 1 to 10 years for equilibration. It is possible that the high-MgO melt inclusions in plagioclase studied by McNeill and Danyushevsky (1996) also record equilibration of initially less MgO-rich melts with this primitive melt via diffusion because this process would not take much more time than the homogenisation of the plagioclase crystal. For example, using the analytical solution for diffusive reequilibration of melt inclusions of Qin et al. (1992) we find that a 25-μm

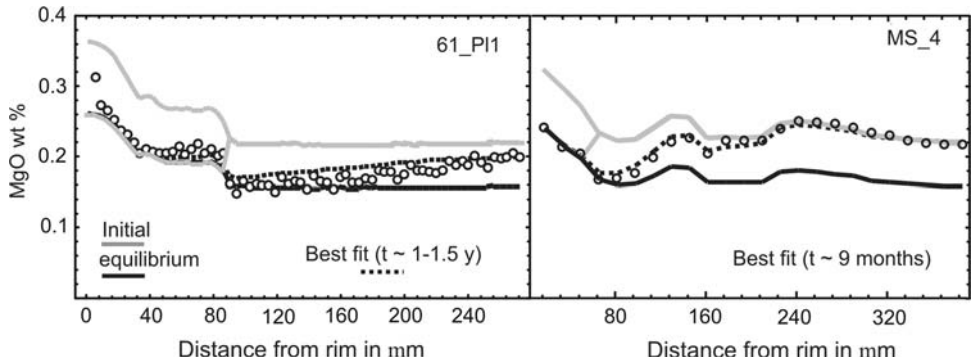

Fig. 8 Results of diffusion models for Mg in the two plagioclase crystals from the samples from Site 648B which show disequilibrium Mg distributions. The models both use two types of initial Mg distribution in the plagioclase. In one case, the core is in equilibrium with a melt containing 11 wt% MgO (the maximum we have calculated; Fig. 5) and the rim with a melt containing ~8 wt% MgO (corresponding approximately to the bulk-rock MgO content). In the other case the entire crystal has an initial distribution at 11 MgO wt%. The two types of initial profiles are used to account for the possible heterogeneity in MgO concentration in the melts of the mush zone. The calculated profiles for the models with the different initial conditions overlap with each other. For crystal 61_pl1 the times vary between 1 and 1.5 years depending on the initial profile, whereas for crystal MS_4 both initial conditions give the same time (a difference of a week). Irrespective of the details, preservation of disequilibrium in the distribution of Mg within this crystal requires that it was brought into contact with the low MgO melt less than a few years prior to eruption

diameter inclusion in the centre of a 1-mm diameter crystal (An_{85}) would equilibrate (to 95%) with a surrounding melt in ~15 years at 1,200°C.

To model the profile of crystal 68_pl1 we have used an initial profile, where the entire plagioclase was in equilibrium with a liquid with 9 wt% MgO which is the lowest value calculated to be in equilibrium with any portion of the crystal. The model sets the MgO content of the rim of the plagioclase crystal to be in equilibrium with a melt with ~12 wt% MgO (the highest melt MgO content in equilibrium with this crystal) and allows Mg to diffuse in from an infinite reservoir of Mg in the melt. Figure 9 shows that the observed MgO distribution in this crystal can be reproduced quite well by allowing diffusion of Mg into the crystal for ~1 year. Thus the high-MgO melt was in contact with this crystal for ~1 year prior to the final mixing event with the more evolved melt that carried this crystal to the surface. This time is longer than the one retrieved for the final mixing event (days) but still shows that the environment is very dynamic, where multiple mixing events can occur within a year.

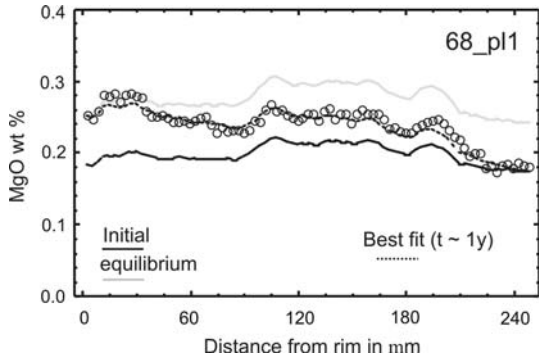

Fig. 9 Results of diffusion model for Mg in crystal 68_pl1. The initial condition for the model is a Mg distribution in equilibrium with the measured core composition. The measured rim composition is used as the boundary condition at the crystal rim. This modelling suggests that ~1 year elapsed between when the MgO-rich melt was brought into contact with this plagioclase crystal and eruption

Discussion

Mixing of an evolved phenocryst-poor magma and a more primitive crystal-bearing magma appears to be a widespread process in the generation of MORB based on the common occurrence of xenocrysts that are more primitive than crystals in equilibrium with their host basalt. The data and modelling presented above provide strong evidence for mixing between a crystal-rich mush zone and a more evolved aphyric magma occurring shortly (years to days) prior to eruption in both locations studied. The short times between magma mixing and eruption support the idea that the arrival of new magma may trigger eruptions at mid-ocean ridges. This situation was proposed by Sinton and Detrick (1992) for slow-spreading ridges which are not underlain by quasi-steady state eruptible magma in melt-dominated lenses and probably require recharge immediately prior to eruption.

Comparison of time scales derived from previous diffusion studies

There have been few studies that have used the extent of diffusive exchange between crystals and their host basalt to investigate the time intervals between mixing events and

eruption at mid-ocean ridges. To our knowledge all previous studies have used the zoning in olivine phenocrysts to try to determine mixing-to-eruption time intervals (Nabeleck and Langmuir 1986; Humler and Whitechurch 1988; Danyushevsky et al. 2002; Pan and Batiza 2002). These studies suggest a range of time intervals from a few years to some days but have generally not focussed on extracting this parameter.

In contrast to the other studies, Pan and Batiza (2002) present models for diffusive exchange between numerous olivine crystals and the melt surrounding them for crystals in basalts from the fast-spreading northern East Pacific Rise (EPR). These results complement those presented here and allow us to investigate whether there is evidence for a spreading rate control on the timescale of 'magma mixing' at mid-ocean ridges. Pan and Batiza (2002) found that most olivine phenocrysts recorded a short time interval between mixing and eruption at the northern EPR of months to years with shorter time intervals being more common than longer ones. These time scales are similar to those found here for magma–mush interaction. In detail, the time scales they find are somewhat shorter than those found by us using plagioclase from the Serocki volcano on the slow-spreading MAR. The shorter times obtained by Pan and Batiza (2002) are partly the result of using the FeMg diffusion coefficient parallel to the *c* axis for all crystals, which is a factor of ~ 6 faster than diffusion parallel to *a* or *b* (e.g. Dohmen and Chakraborty 2007).

Whether there is a spreading rate control on the rates of mixing and eruption is unclear at present because: (1) olivine may record a different history to plagioclase due to its greater density and hence the likely preferential entrainment of plagioclase from a mush zone; (2) there is no clear change in post-mixing residence time with spreading rate between the intermediate spreading Costa Rica Rift and the fast-spreading EPR; and (3) there is evidence that multiple mixing events occurred in all locations. Future studies that apply the approach developed herein, ideally along with similar studies of olivine crystals, should allow a robust evaluation of whether there is a spreading rate control on the interval between the last mixing event and eruption at mid-ocean ridges globally. It is already clear, however, that mixing occurs repeatedly during the petrogenesis of MORB at all spreading rates and the last mixing event commonly occurs within less than a year of eruption.

Comparison of time scales from diffusion modelling with ^{210}Pb disequilibria and the role of interstitial melt from a crystal mush in controlling MORB geochemistry

Rubin et al. (2005) report ^{210}Pb ($t_{1/2} = 22$ years) deficits in MORB from intermediate- to fast-spreading ridges which demonstrate that Ra–Pb fractionation occurs within the MORB system. This deficit is largest in the most primitive samples (e.g. highest MgO and Ni). They propose that this fractionation occurs within the mantle and hence suggest that melts can be erupted within decades of being generated within the mantle. As an alternative, Van Orman and Saal (2007), following Saal and Van Orman (2004) and Van Orman et al. (2006), suggest that diffusive exchange between interstitial melt and crystals within a crystal mush zone in the crust may lead to ^{210}Pb depletion in the melt. Studies of oceanic gabbros have provided evidence of melt-rock reaction with a crystal mush zone in the crust (e.g. Dick et al. 1991; Coogan et al. 2000) but whether this interstitial melt could impact the composition of erupted MORB has been unclear.

Our data support the idea that disaggregation of a crystal mush zone, in which crystal-melt reaction has previously occurred, is common at mid-ocean ridges (c.f. Sinton et al. 1993; Ridley et al. 2006) allowing the interstitial melt (as well as crystals) to be incorporated into the melt that is erupted. Mixing a small amount of primitive (high MgO) interstitial melt with a low ^{210}Pb/^{226}Ra activity ratio generated in this manner (~ 0.1 based on Van Orman and Saal 2007) with a larger volume of more evolved melt with no ^{210}Pb/^{226}Ra disequilibria could potentially generate the ^{210}Pb/^{226}Ra disequilibria observed by Rubin et al. (2005; ^{210}Pb/^{226}Ra activity ratios mainly between 0.9 and 1.0). Critically our observations show that disaggregation of a crystal mush commonly occurs shortly before eruption which will prevent in situ ^{210}Pb decay eradicating this signature in the mixed (erupted) magma.

Conclusions

The main conclusions of this study are:

- Analysis of compositional zoning in plagioclase phenocrysts in two different MORB suites demonstrates that crystals are exposed to repeatedly changing chemical and physical environments on short (years to decades) time scales. The observations are most readily explained if plagioclase phenocrysts are commonly derived from a pre-existing crystal mush zone shortly before eruption.
- The process of disaggregation of a crystal mush means that the interstitial melt in the mush zone must play a role in controlling the composition of the erupted basalts—effectively enhancing the role of in situ crystallisation (Langmuir 1989). This may also have important consequences for the interpretation of U-series disequilibria in MORB (Saal and Van Orman 2004; Van Orman et al. 2006; Van Orman and Saal 2007).

- Plagioclase crystals record evidence of the involvement of melts with ≥11 wt% MgO—more magnesian than any erupted MORB—in the petrogenesis of both sample suites. These primitive melts may be commonly transported to shallow levels in a mush zone but never erupted due to ubiquitous mixing with more evolved melts.

Acknowledgments Reviews by J. Sinton and P. Wallace are greatly appreciated and helped to clarify various parts of the manuscript. FC acknowledges contracts under project 526 of the German Science Foundation and a Ramon y Cajal Fellowship Spanish Ministry of Education. The ocean drilling program is acknowledged for providing access to the samples studied here. NSERC funded the LA-ICP-MS analyses at the University of Victoria.

References

Albarede F, Bottinga Y (1972) Kinetic disequilibrium in trace element partitioning between phenocryst and host lava. Geochim Cosmochim Acta 35:141–256

Alt JC, Kinoshita H, Stokking LB et al (1993) Proceedings of ODP, initial reports, vol 148. College Station, TX (Ocean Drilling Program)

Bindeman IN, Davis AM, Drake MJ (1998) Ion microprobe study of plagioclase-basalt partition experiments at natural concentration levels of trace elements. Geochim Cosmochim Acta 62:1175–1193

Blundy JD, Wood BJ (1991) Crystal-chemical controls on the partitioning of Sr and Ba between plagioclase feldspar, silicate melts, and hydrothermal solutions. Geochim Cosmochim Acta 55:193–209

Brewer TS, Bach W, Furnes H (1996) Geochemistry of lavas from Hole 896A. In: Alt JC, Kinoshita H, Stokking LB, Michael PJ (eds) Proceedings ocean drilling program scientific results, vol 148, pp 9–17

Cashman K (1990) Textural constraints on the kinetics of crystallization of igneous rocks. Rev Mineral 24:259–314

Cashman K (1993) Relationship between plagioclase crystallization and cooling rate in basaltic melts. Contrib Mineral Petrol 113:126–142

Cherniak DJ, Watson EB (1994) A study of strontium diffusion in plagioclase using Rutherford backscattering spectroscopy. Geochim Cosmochim Acta 58:5179–5190

Coogan LA, Saunders AD, Kempton PD, Norry MJ (2000) Evidence from oceanic gabbros for porous melt migration within a crystal mush beneath the Mid-Atlantic Ridge. Geophys Geochem Geosys 1: Paper No 2000GC000072

Costa F, Chakraborty S, Dohmen R (2003) Diffusion coupling between major and trace elements and a model for the calculation of magma chamber residence times using plagioclase. Geochim Cosmochim Acta 67:2189–2200

Costa F, Dohmen R, Chakraborty S (2008) Time scales of magmatic processes from modeling the zoning patterns of crystals. Rev Mineral Geochem 69:545–594

Crank J (1975) The mathematics of diffusion. Oxford Science Publications

Danyushevsky LV, Sokolov S, Falloon TJ (2002) Melt inclusions in olivine phenocrysts: using diffusive re-equilibration to determine the cooling history of a crystal, with implications for the origin of olivine-phyric volcanic rocks. J Petrol 43:1651–1671

Dick HJ, Meyer SH, Bloomer S, Kirby D, Stakes, Mawer C (1991) Lithostratigraphic evolution of an in situ section of oceanic layer 3. In: Von Herzen PR et al (ed) Proceedings of the ocean drilling program Leg 118, Scientific Results. U.S. Government Printing Office, Washington, pp 439–540

Dohmen R, Chakraborty S (2007) Fe–Mg diffusion in olivine II: point defect chemistry, change of diffusion mechanisms and a model for calculation of diffusion coefficients in natural olivine. Phys Chem Min 34:409–430

Donaldson CH, Brown RW (1977) Refractory megacrysts and magnesium-rich melt inclusions within spinel in oceanic tholeiites: indicators of magma mixing and parental magma composition. Earth Planet Sci Lett 37:81–89

Dungan MA, Rhodes JM (1978) Residual glasses and melt inclusions in basalts from DSDP Leg 45 and 46: evidence for magma mixing. Contrib Mineral Petrol 67:417–431

Dungan M, Long PE, Rhodes JM (1978) The petrography, mineral chemistry, and one-atmosphere phase relations of basalts from Site 395. In: Melson WG, Rabinowitz PD et al (eds) Initial reports of the deep sea drilling project. US Government Printing Office, Washington, pp 461–477

Fisk M, McNeill AW, Teagle DAH, Furnes H, Bach W (1996) Data report: major-element chemistry of Hole 896A glass. In: Alt JC, Kinoshita H, Stokking LB, Michael PJ (eds) Proceedings of ocean drilling program scientific results, vol 148, pp 483–487

Flower MJF, Robinson PT, Schmicnke H-U, Ohnmacht W (1977) Petrology and geochemistry of igneous rocks, DSDP Leg 37. DSDP Init Rep 37:653–679

Ghiorso MS, Sack RO (1995) Chemical mass transfer in magmatic processes. IV. A revised and internally consistent thermodynamic model for the interpolation and extrapolation of liquid–solid equilibria in magmatic systems at elevated temperatures and pressures. Contrib Mineral Petrol 119:197–212

Giletti BJ, Casserly JED (1994) Strontium diffusion kinetics in plagioclase feldspars. Geochim Cosmochim Acta 58:3785–3797

Goldstein SJ, Perfit MR, Batiza R, Fornari DJ, Murrell MT (1994) 226Ra and 231Pa systematics of axial morb, crustal residence ages, and magma chamber characteristics at 9–10°N East Pacific Rise. Min Mag 58:335–336

Grove TL, Baker MB, Kinzler RJ (1984) Coupled CaAl–NaSi diffusion in plagioclase feldspar: experiments and applications to cooling rate speedometry. Geochim Cosmochim Acta 48:2113–2121

Grove TL, Kinzler RJ, Bryan WB (1990) Natural and experimental phase relations of lavas from Serocki volcano. In: Detrick R, Honnorez J, Bryan WB, Juteau T et al (eds) Proceedings of ocean drilling program scientific results, vol 106/109, pp 9–17

Grove TL, Kinzler RJ, Bryan WB (1992) Fractionation of Mid-Ocean Ridge Basalt (MORB), In: Morgan JP, Blackman DK, Sinton JM (eds) Mantle flow and melt generation at Mid-Ocean Ridges. AGU Geophysical Monograph, vol 71, pp 281–310

Hammer J (2008) Experimental studies of the kinetics and energetics of magma crystallization. Rev Min Geochem 69:9–59

Horn I, Hinton RW, Jackson SE, Longerich HP (1997) Ultra-trace element analysis of NIST SRM 616 and 614 using laser ablation microprobe inductively coupled plasma mass spectrometry (LAM-ICP-MS): a comparison with secondary ion mass spectrometry (SIMS). Geostand Newsl 21(2):191–203

Humler E, Whitechurch H (1988) Petrology of basalts from the Central Indian Ridge (lat. 25 23′S, long. 70 04′E): estimates of frequencies and fractional volumes of magma injections in a two layered reservoir. Earth Planet Sci Lett 88:169–181

Klein EM, Langmuir CH (1987) Global correlation of ocean ridge basalt chemistry with axial depth and crustal thickness. J Geophys Res 92:8089–8115

Kuo L-C, Kirkpatrick RJ (1982) Pre-eruption history of phyric basalts from DSDP Legs 45 and 46: evidence from morphology and zoning patterns in plagioclase. Contrib Mineral Petrol 79:13–27

Langmuir CH (1989) Geochemical consequences of in situ differentiation. Nature 340:199–205

Langmuir CH, Klein EM, Plank T (1992) Petrological systematics of Mid-Ocean ridge basalts: constraints on melt generation beneath ocean ridges. In: Morgan JP, Blackman DK, Sinton JM (eds) Mantle flow and melt generation at Mid-Ocean Ridges. AGU Geophysical Monograph, vol 71, pp 183–280

LaTourrette T, Wasserburg GJ (1998) Mg diffusion in anorthite: implications for the formation of early solar system planetesimals. Earth Planet Sci Lett 158:91–108

Lesher CE (1994) Kinetics of Sr and Nd exchange in silicate liquids: theory, experiments, and applications to uphill diffusion, isotopic equilibration, and irreversible mixing of magmas. J Geophys Res 99:9585–9604

McNeill AW, Danyushevsky LV (1996) Composition and crystallization temperatures of primary melts from hole 896A basalts: evidence from melt inclusion studies. In: Alt JC, Kinoshita H, Stokking LB, Michael PJ (eds) Proceedings of ocean drilling program scientific results, vol 148, pp 21–35

Meyer PS, Shibata T (1990) Complex zoning in plagioclase feldspars from ODP site 648. In: Detrick R, Honnorez J, Bryan WB, Juteau T et al (eds) Proceedings of ocean drilling program scientific results, vol 106/109, pp 123–142

Nabeleck PI, Langmuir CH (1986) The significance of unusual zoning in olivines from FAMOUS area basalt 527-1-1. Contrib Mineral Petrol 93:1–8

Pan Y, Batiza R (2002) Mid-ocean ridge magma chamber processes: constraints from olivine zonation in lavas from the East Pacific Rise at 9°30′N and 10°30′N. J Geophys Res 107. doi10.1029/2001JB000435

Pearce NJG, Perkins WT, Westgate JA, Gorton MP, Jackson SE, Neal CR, Chenery SP (1997) A compilation of new and published major and trace element data for NIST SRM 610 and NIST SRM 612 glass reference materials. Geostand Newsl 21:115–144

Perk N, Coogan LA, Karson JA, Klein EM, Hanna H (2007) Primitive cumulates from the upper crust formed at the East Pacific Rise. Contrib Mineral Petrol 154:575–590

Presnall DC, Hoover JD (1987) High pressure phase equilibrium constraints on the origin of mid-ocean ridge basalts. Geochem Soc (Spec paper no. 1):75–89

Qin Z, Lu F, Anderson AT (1992) Diffusive reequilibration of melt and fluid inclusions. Am Min 77:565–576

Ridley WI, Perfit M, Smith MC, Fornari DJ (2006) Magmatic processes in developing oceanic crust revealed in a cumulate xenoliths collected at the East Pacific Rise, 9°50′N. Geochem Geophys Geosys 7. doi:10.1029/2006GC001316

Rubin KH, van der Zandler I, Smith MC, Bergmanis EC (2005) Minimum speed limit for ocean ridge magmatism from ^{210}Pb–^{226}Ra–^{230}Th disequilibria. Nature 437:534–538

Saal AE, Van Orman JA (2004) The 226Ra enrichment in oceanic basalts: evidence for melt-cumulate diffusive interaction processes within the oceanic lithosphere. Geochem Geophys Geosys 5. doi:10.1029/2003GC000620

Sato H, Aoki K-I, Okamoto K, Fujita B-Y (1979) Petrology and chemistry of Basaltic rocks from Hole 396B, IPOD/DSDP Leg 46. DSDP Init Rep 46:115–141

Shipboard Scientific Party (1988) Site 648. In: Detrick R, Honnorez J, Bryan WB, Juteau T et al (eds). Proceedings of ODP, initial reports, vol 106/109. College Station, TX (Ocean Drilling Program)

Sinton JM, Detrick RS (1992) Mid-Ocean Ridge magma chambers. J Geophys Res 97:197–216

Sinton CW, Christie DM, Coombs VL, Nielsen RL, Fisk MR (1993) Near-primary melt inclusions in anorthite phenocrysts from the Galapagos Platform. Earth Planet Sci Lett 119:527–537

Smith VG, Tiller WA, Rutter JW (1955) A mathematical analysis of solute redistribution during solidification. Can J Phys 33:723–745

Van Orman JA, Saal AE (2007) Reconciling Pb-210 deficits with the physics of melt extraction. Geochim Cosmochim Acta 71:A1058

Van Orman JA, Saal AE, Bourdon B, Hauri EH (2006) Diffusive fractionation of U-series radionuclides during mantle melting and shallow level melt-cumulate interaction. Geochim Cosmochim Acta 70:4797–4812